Pure Appl. Chem., Vol. 81, No. 4, pp. 635–647, 2009.
doi:10.1351/PAC-CON-08-09-11

Photochemical routes to silver and gold nanoparticles*

Juan C. Scaiano‡, Paul Billone, Carlos M. Gonzalez, Luca Maretti, M. Luisa Marin, Katherine L. McGilvray, and Nathan Yuan

Department of Chemistry, University of Ottawa, 10 Marie Curie, Ottawa, Ontario K1N 6N5, Canada

Abstract: The photochemistry of aromatic ketones through the Norrish type I cleavage of benzoins and via photoreduction generates ketyl radicals that readily reduce many metal ions, including silver and gold. Reduction to Au(0) and Ag(0) leads to the spontaneous formation of nanoparticles (NPs) in aqueous or micellar solutions. Careful consideration of kinetic factors to minimize triplet quenching by metal ions can lead to rapid NP generation. These materials are quite stable and have interesting reactivities due to the essentially unprotected characteristics of the surface.

Keywords: nanomaterials; nanoparticles; photochemistry; benzophenone; particle synthesis.

INTRODUCTION

This article deals with the use of photochemical methodologies for the synthesis of metal nanoparticles (NPs), particularly Au and Ag, and centers on contributions from our research group. Many group members, past and present, have contributed material, and their names appear in the references; it is coauthored by current group members whose recent contributions are emphasized in this article; in a few cases, we have also included unpublished material.

Photochemistry is an attractive tool for the preparation of nanomaterials because of the spatial and temporal control that these techniques normally possess. Thus, the implementation of imaging and lithographic applications [1] is relatively straightforward when light is an essential ingredient for the generation of nanostructures. Similarly, some health-related potential applications can benefit from the ready control of the generation, transmission, and delivery of light.

The vast majority of methodologies for the synthesis of metal NPs rely on the metal ions as starting materials, and thus suitable reducing agents are required. In thermal methods, the use of reducing agents such as sodium borohydride is common [2]. Just as in the case of thermal methods photochemistry also depends on the generation of reducing species in the photodecomposition of carefully selected molecules. Ideally, these molecules do not contain the reducing moiety before they are photoexcited, since their presence in the ground state would limit the opportunities for spatial and temporal control. In the examples discussed in this contribution, the preferred reducing species are free radicals.

Interestingly, in some cases it is possible to use the photosensitizer as a catalytic material that is regenerated after mediating free radical formation. These examples are reminiscent of related applications of photochemistry that have been referred to as "positive photocatalysis" [3] to differentiate them

*Paper based on a presentation at the 19th International Conference on Physical Organic Chemistry (ICPOC-19), 13–18 July 2008, Santiago de Compostela, Spain. Other presentations are published in this issue, pp. 571–776.

‡Corresponding author

from the frequent use of photochemistry for the destruction of organic molecules in environmental applications.

PHOTOCHEMICAL STRATEGIES

Among the many types of radicals with well-established properties, ketyl and α-aminoalkyl radicals are excellent reducing agents and are easy to produce photochemically [4,5]. In our laboratory we have generally preferred ketyl radicals [6], largely because precursors of α-aminoalkyl radicals contain the amine function that in some cases, such as Au(III) and Au(I), can lead to a slow thermal reduction that limits the shelf life of solutions; while this is not a serious problem in the research laboratory, it would limit possible commercial applications of these methodologies. However, in cases where reduction by ketyl radicals is a "reluctant" process, α-aminoalkyl radicals offer an alternative strategy; we comment on one such case later in this paper.

Scheme 1 shows three of the photoreactions that can be employed for the generation of ketyl radicals from organic molecules.

A: Photoreduction

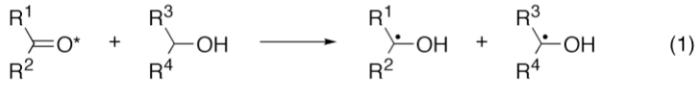

B: Norrish Type I cleavage

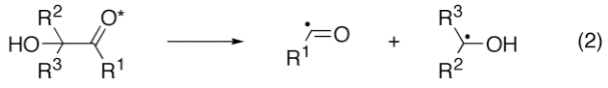

C: Pinacol Photocleavage

Scheme 1 Photochemical strategies for the generation of ketyl radicals from organic precursors. The asterisk (*) denotes the excited state of a molecule, frequently a triplet state in the examples used in this contribution, while "hν" indicates exposure to light. The symbols R^1 to R^4 represent organic moieties, most commonly alkyl, aryl, or H-atom.

Reaction **A** in Scheme 1 has been written as a C–H hydrogen abstraction from an alcohol, although reaction of the excited ketone with other hydrogen donors, such as hydrocarbons, is also possible [7]. In this case, only one ketyl radical is formed (vide infra). While reaction **C** represents a very "clean" source of ketyl radicals, we have not explored it, largely because common pinacols absorb light at relatively short wavelengths in the UV region, where competitive absorption by the metal precursor is frequently unavoidable.

Benzoins as ketyl precursors

The Norrish type I reaction can occur from both singlet and triplet excited state, but in the case of aromatic ketones (R^1 = aryl) it is dominated by triplet state reactions [8,9]. This cleavage is not specific to

benzoins (i.e., containing the alcohol functionality), although in this case it generates ketyl radicals, and is in many cases remarkably fast. Scheme 2 shows a few of the structures that have been used for NP synthesis in our research group.

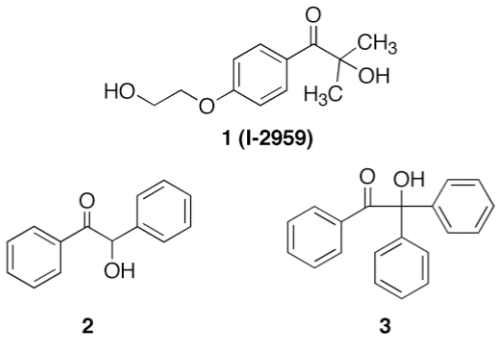

Scheme 2 Examples of benzoins that were used in our laboratory. Compound **1** is sold commercially as Irgacure-2959™ and is the only one in this chart that is readily soluble in water.

Compound **1** has been a favorite in our group, being readily available, water-soluble, and producing ketyl radicals with a quantum yield of 0.29 in fast photocleavage from a triplet state with a lifetime of just 11 ns [9].

Ketone photoreduction as a precursor for ketyl radicals

With over a century of research in this field, ketone photoreduction is a classic example in photochemistry and one of the best understood photochemical reactions. In the case of benzophenone, its triplet state has n,π* character, a property that makes it an excellent hydrogen abstractor from appropriate donors (such as alcohols, some hydrocarbons, benzylic and allylic hydrogens, among others), as illustrated in Scheme 3 [7,10].

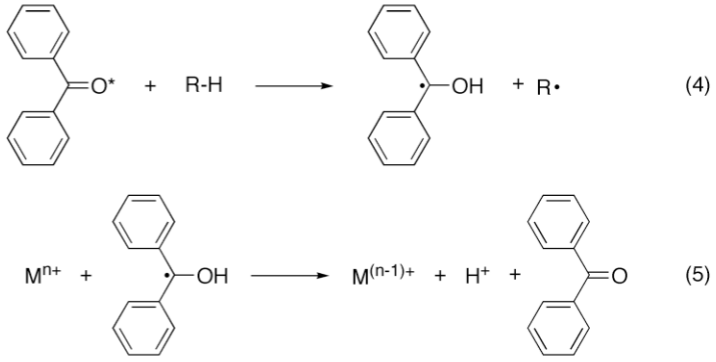

Scheme 3 Photoreduction of benzophenone followed by electron transfer to the metal ion M^{n+}.

Reaction 5 in Scheme 3 serves to emphasize the catalytic nature of the process, since benzophenone is regenerated, in contrast with systems involving benzoin where the starting ketone is not regenerated in the process. Ketyl radicals are one-electron reducing agents, something that must be taken into consideration when multielectron processes are involved, such as in the case of Au(III). Note that

acid is also generated in the reaction, and thus when working with unbuffered millimolar solutions it is common to have pH ~ 3 at the end of the reaction.

Au NANOPARTICLES

The most common precursor for Au nanoparticles (AuNPs) is $HAuCl_4$ or its salts. The Turkevich [11] and Brust–Schiffrin [2] methods using citrate and $NaBH_4$ as reducing agents, respectively, are widely used. The latter makes small particles that owe their stability to the surface derivatization with thiols.

We have found that AuNPs can be readily prepared by irradiating in the UVA region (315–400 nm) a solution of **I-2959** and $AuCl_4^-$; the reaction was remarkably fast, with complete conversion of millimolar solutions in just a few minutes under typical exposure conditions involving irradiances around 40 W/m^2; Figure 1 shows an example of the growth of the surface plasmon band (SPB) at ~530 nm, the characteristic position for approximately spherical AuNPs. Using this methodology we have been able to make AuNPs ranging in diameter from 8 to 40 nm, with their average size

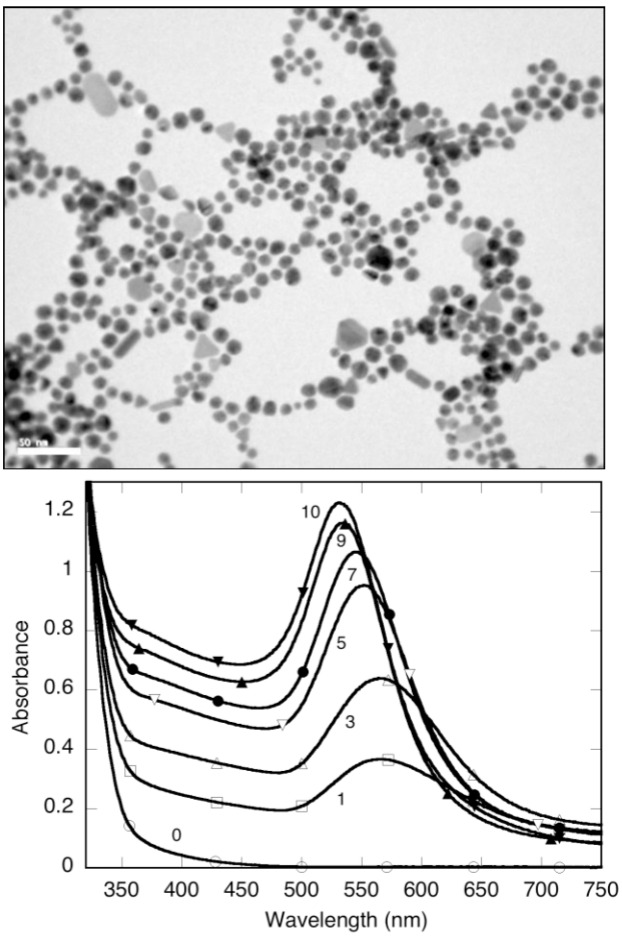

Fig. 1 TEM of AuNPs (top, 30 min exposure) and absorbance over time (bottom) for a solution of 1 mM **I-2959** and 0.3 mM $AuCl_4^-$ irradiated in well plate under air, with the spectra recorded 16 h after UVA exposure. The numbers next to each trace indicate the exposure time in minutes.

being a function of the irradiance employed, with higher irradiances leading to smaller particles [6]; we anticipate that a broader range would be accessible by suitable adjustment of the exposure conditions.

Interestingly, AuNPs can be readily prepared under an inert atmosphere (N_2 or Ar), as well as under air or oxygen. The presence of oxygen in the aqueous solution leads to a short induction period, indicative of the sacrificial use of some of the radicals in the system to consume the dissolved oxygen, as shown in reaction 6 for the case of the corresponding ketyl radical [6]. We note that these irradiations are performed in unstirred solutions and that therefore dissolved oxygen is unlikely to be replenished during the short irradiation periods.

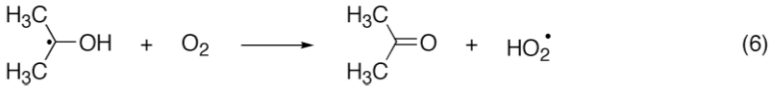

(6)

The particles prepared in this manner are stable essentially indefinitely (>6 months) when preserved in plastic or fused silica containers, with no need for added surface stabilizers [6]. The particles are probably not "naked", since such a colloidal solution would be unlikely to show long-term stability; however, these AuNPs do not have any covalently bound stabilizers. We assume that chloride and possibly species derived from the substituted benzoyl radical produced from **I-2959** contribute to this stability. Consistent with this, the AuNPs prepared by this method systematically show negative zeta potentials, frequently in the –20 to –40 mV range, large enough to prevent colloidal aggregation.

The efficiency and rate of AuNP formation is remarkable given that Au(III) (added as $AuCl_4^-$) quenches aromatic ketone triplets with rate constants approaching diffusion control (e.g., about 10^{10} M^{-1} s^{-1} for the azaxanthone triplet); this rapid quenching is the root of the frequently reported long exposure times for photochemical NP synthesis. In this particular system, the rapid Norrish type I cleavage (τ_T ~ 11 ns) [9] results in minimal triplet quenching, in spite of the high rate constant for this process.

Synthesis of AuNPs in micellar solution

Ketones **2** and **3** (see Scheme 2) are also excellent ketyl radical precursors and undergo triplet cleavage in adequately short times, so that quenching by Au(III) is not a problem. In particular, **3** is an excellent mechanistic tool, since it yields the same ketyl radical as benzophenone (see Scheme 3), an intermediate that is well characterized and that can be readily monitored using laser flash photolysis techniques. In independent studies, we have established that electron transfer to Au(III) occurs with a rate constant of ~10^9 M^{-1} s^{-1} [12].

Given the hydrophobic nature of **2** and **3**, AuNP synthesis was carried out in micellar systems, with cetyltrimethylammonium chloride (CTAC) as the surfactant of choice. Again, AuNPs were very stable and their synthesis could be achieved in just a few minutes.

One of the applications of **3** as a mechanistic tool is illustrated in Fig. 2, where one of these mechanistic applications is evident. Thus, **3** has a much weaker absorption in the 300–400 nm region than **1**, and allows the recording of the disappearance of the $HAuCl_4$ at about 330 nm. If we look closely at the data after 3 min exposure we realize that over 80 % of Au(III) has been consumed, while only about 5 % of the SPB (based on the final absorbance) has been formed. At this point in time the Au ions are mainly present as Au(I), which largely accumulates before the final reduction to Au(0) takes place [13].

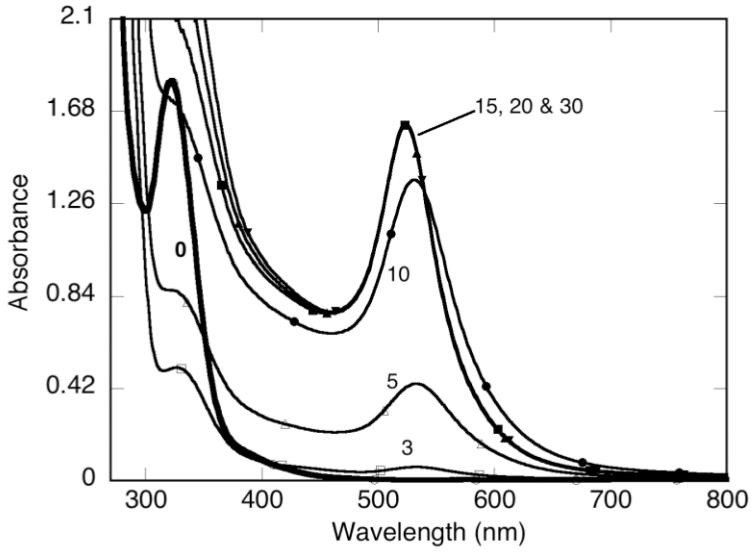

Fig. 2 Absorbance of AuNPs over time for a solution of 1 mM **3** and $AuCl_4^-$ containing 66 mM CTAC under air, with the spectra after UVA exposure. The numbers next to each trace indicate the exposure time in minutes.

The three-electron reductive processes that lead to Au(0) and from it to AuNP are summarized in Scheme 4. Note that Au(II) is quite unstable and readily disproportionates, and thus reduction of Au(II) to Au(I) by ketyl radicals is not included, even if it is thermodynamically feasible. On the other hand, disproportionation of Au(I) is slow and the final reductive process likely involves ketyl radicals [6,13].

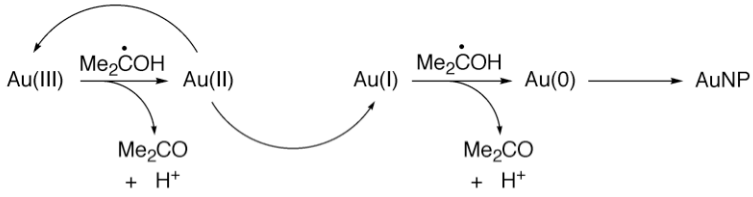

Scheme 4 Reductive processes leading to Au(0) and AuNP.

Ag NANOPARTICLES

Ag nanoparticles in micellar solution

In a recent study on silver nanoparticles (AgNPs) we were interested in examining the effect of external magnetic fields on the reductive processes leading to AgNPs [14]. While aspects relating to magnetic field effects are beyond the scope of this article, the approach employed to reduce excited-state quenching by Ag^+ forms an integral part of the strategies discussed here. In this case, the ketyl radicals were generated from benzophenone in micellar solution [15] according to the photocatalytic processes of Scheme 3, where $M^+ = Ag^+$.

Ag cations quench benzophenone triplets with a rate constant of 4.6×10^9 M^{-1} s^{-1} in sodium dodecyl sulfate (SDS) micellar solution [14]. When RH in Scheme 3 is the surfactant, hydrogen abstraction occurs from the CH_2 moieties in SDS. While the micelles offer "segregation" of the benzophenone and the metal ions (i.e., benzophenone in the micelles and Ag^+ in the aqueous phase) considerable

quenching still occurs, since Coulombic interactions probably result in Ag^+ being a counterion to the anionic micelle. The system needs to be biased in favor of photoreduction and at the expense of triplet-state quenching. This was achieved by adding 1,4-cyclohexadiene as a hydrogen donor; this molecule has exceptional hydrogen donor abilities due to the presence of four double-allylic hydrogens [16,17]; further 1,4-cyclohexadiene is also rather hydrophobic and if desired can be readily eliminated from the system given its high vapor pressure.

Thus, in this system it is also possible to prepare AgNPs in just a few minutes by combining spatial segregation strategies and the addition of a good hydrophobic hydrogen donor. AgNPs formed in this manner showed the characteristic SPB at around 410 nm.

Fluorescent Ag nanoparticles

Given the success in generating AuNPs using **I-2959** as radical generator, we explored the possibility of using this ketone to make AgNP. Beyond making aqueous AgNP, we examined whether **I-2959** could be employed in nonaqueous media, since this useful molecule has some solubility in a wide range of organic solvents as well as in micellar systems. Using $AgCF_3COO$ as a precursor and in the presence of cyclohexylamine in tetrahydrofuran (THF), the photogenerated ketyl radicals lead to the formation of small AgNPs within minutes. Transmission electron microscopy (TEM) reveals particles of about 3.4 nm in diameter, and ^{19}F NMR studies show the presence of fluorine (as CF_3COO^-) on the NP surface. Much to our surprise these particles are strongly fluorescent, with λ_{max} ~ 582 nm in THF.

While TEM only reveals pure metallic AgNPs, it would be unreasonable to assume that this emission arises from the corresponding SPB, since the nature of plasmon transitions is such that they are not expected to lead to luminescence. The luminescence seems consistent with the presence of small Ag clusters, specifically Ag_2 and Ag_3, both known to be fluorescent in this spectral region [18,19]. At this point, we believe that these clusters are located on the surface of the NPs detected by TEM, but cannot rule out the presence of free, stabilized Ag_2 in solution; further work on this topic will be reported elsewhere [12].

From the point of view of this contribution, the example above shows clearly the wide applicability of the photochemical strategies described here.

CORE-SHELL Au/Ag NANOPARTICLES

In order to further explore the potential of the strategies developed using the chemistries shown in **A** and **B** in Scheme 1, we also examined the possibility of preparing bimetallic NPs. Au/Ag core-shell particles for which there is already significant information in the literature [20] seemed a reasonable test system. Given a mixture of Ag(I) and Au(III), one expects and observes that Au is reduced first, something that is anticipated both from the redox potentials and from the simple fact that Au is a "more noble metal" than Ag. The fact that Ag requires only one electron, while Au takes the stepwise delivery of three electrons is not enough to overcome redox characteristics, and as a result the simultaneous reduction of Ag/Au mixtures leads to the initial formation of AuNPs with Ag deposited late in the reaction and largely on the surface. Thus, these NPs usually have a Au core and a Ag shell. Spectra of these particles and some of their interesting dissolution properties are shown later in this report (vide infra).

Au/Ag bimetallic core-shell NPs generally show two distinguishable plasmon bands; in the case of equimolar systems (i.e., $x_{Ag} \approx x_{Au}$, where "x" stands for mole fraction) the Ag SPB is around 400 nm, while that for Au is blue-shifted with respect to the case of pure AuNP, for example, when prepared in CTAC micelles we observed this maximum at ~490 nm, compared with ~525 nm in AuNP.

As in earlier examples, the synthesis of bimetallic NPs by this method serves to illustrate well the versatility of the strategies of Scheme 1. We will later show some of the special properties of these largely unprotected nanomaterials.

THE QUESTION OF STRATEGY

The examples above show that the ketone photoreactions of Schemes 1 and 3 are excellent methodologies for the synthesis of a wide range of metal NPs; key issues are the ketone's ability to generate radicals while avoiding quenching by the metal ions, strategies that are summarized in Fig. 3. Most important, we note that

> Ketones are good photosensitizers for nanoparticle synthesis not because of the energy they can absorb or deliver, but rather because of the reducing free radicals they can generate.

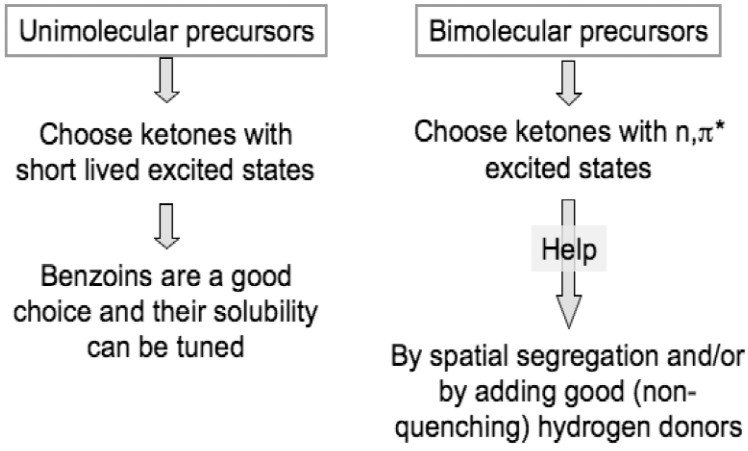

Fig. 3 Photochemical strategies for the synthesis of metal NPs from ketones capable of producing ketyl radicals (see Schemes 1 and 3).

INTERESTING PROPERTIES OF (ALMOST) UNPROTECTED METAL NANOPARTICLES

The photochemical NP synthesis approaches described above efficiently produce particles that are largely unprotected, and in all the examples there are no covalently bound surface stabilizers. As a result, we expect the surface to me more "exposed" than in more common, heavily stabilized nanostructures. In this section, we provide some examples that illustrate these special properties.

Facile derivatization

AuNPs prepared from aqueous solutions of **I-2959** and $AuCl_4^-$ can be easily functionalized on demand with both water-soluble and organic thiols. Upon addition of 3-mercapto-1-propanesulfonic acid sodium salt (MPSA), AuNPs display an SPB that tends to red-shift and diminish in intensity upon increasing the concentration (Fig. 4, top). The growth of a longitudinal plasmon peak around 600 nm is characteristic of nanorod formation and/or moderate flocculation due to the change in ionic strength in the medium. In the case of longer-chain alkanethiols such as 16-mercaptohexadecanoic acid (MHDA), functionalization in a water/ethanol solution leads to simple NP precipitation at increasing concentration, where the NPs are later solubilized following either addition of NaOH to solubilize the bound lig-

ands (not shown) or via resuspension in a polar solvent such as THF or acetonitrile. Figure 4 (bottom) displays an increase in SPB intensity with increasing concentration of MHDA-bound to AuNP in acetonitrile; a higher concentration of thiols leads to a greater degree of stabilization of AuNP in the organic solvent; the reversal between 0.8 and 0.9 mM samples is probably due to experimental error as the particles need to be separated and resuspended in the organic solvent.

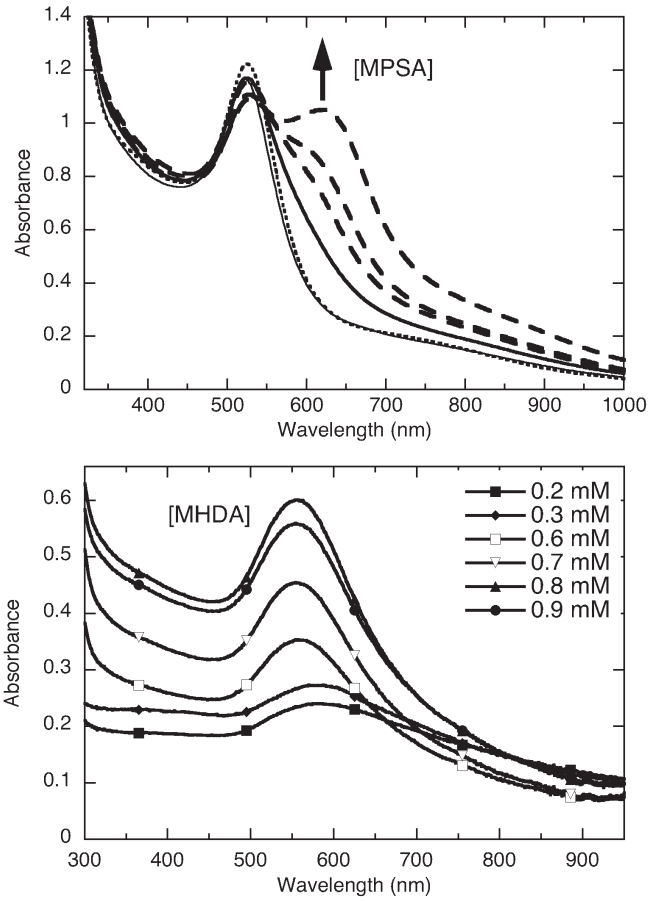

Fig. 4 Absorbance of AuNPs after addition of MPSA (top) and MHDA. AuNPs made from 0.33 mM $HAuCl_4$, 1.0 mM **I-2959**. The concentrations are 0–0.33 mM for MPSA and 0–0.9 mM for MHDA. Bottom panel shows absorbance of AuNPs functionalized with MHDA after centrifugation and resuspension in acetonitrile. Top panel shows aqueous data modified in the same solution in which the AuNPs were prepared; reproduced with permission from the American Chemical Society [6].

Enhanced seeding properties of unprotected AuNPs

The thermodynamic properties of solutions of $HAuCl_4$ and hydroxylamine are such that formation of Au(0), and from it AuNPs should be favorable; yet, the process is kinetically controlled and these solutions have considerable stability (days). Adding to the system AuNP as seeds triggers the reduction, and the process can be easily monitored in real time by following the growth of the SPB, as illustrated in Fig. 5. Our experiments show that AuNPs stabilized with various thiols react slowly, and after 20 min the reaction has barely started (conversion ≤ 10 %). In contrast, in the case of unprotected NPs (prepared in aqueous $HAuCl_4$ and **I-2959**) the reaction is complete within 60 s. Clearly, the surface of fresh

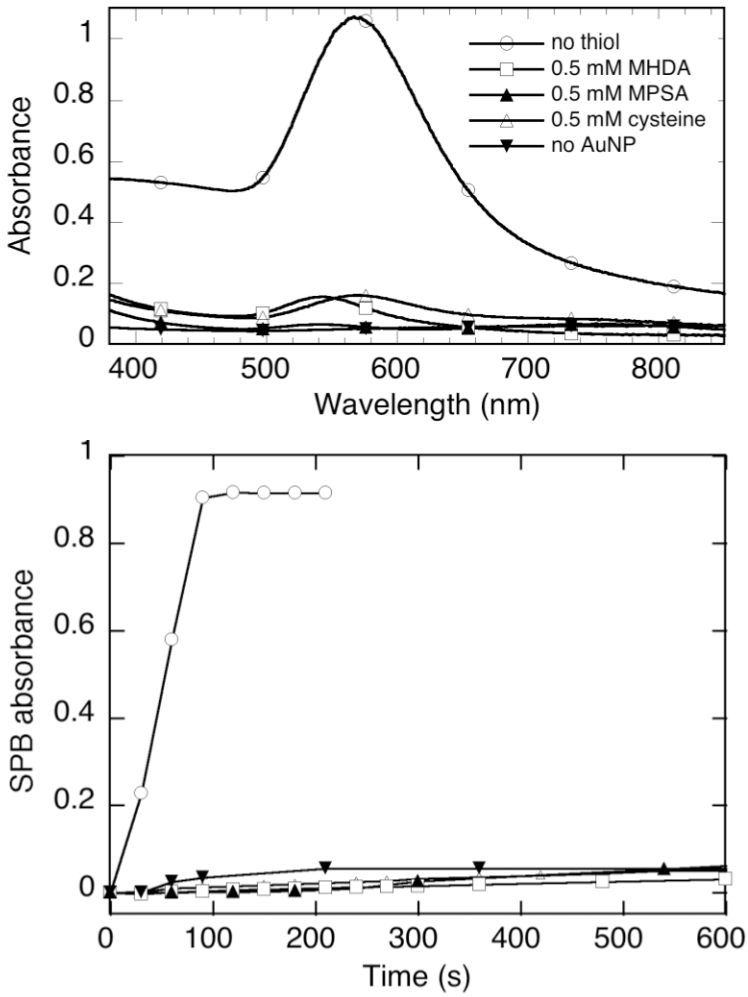

Fig. 5 Growth of the SPB for a sample containing 0.26 mM $HAuCl_4$ and 0.4 mM NH_2OH hydrochloride seeded with AuNP derivatized with various thiols or "unprotected". The AuNP seed was equivalent to a 10 μM solution [based on Au(0)]. Top: spectra after 120 s. Bottom: SPB growth. The same symbols are used in both panels.

unprotected AuNPs is a much better catalyst for reduction of $HAuCl_4$ by hydroxylamine than the surface-protected nanomaterials.

Etching of nanoparticles

Just as shown above in the case the growth of AuNPs, the surface properties of unprotected or lightly protected particles lead to interesting behavior, which we illustrate below with two examples, one involving the etching of AuNP, and the other the dissolution of the Ag shell in Au/Ag core-shell NPs.

Etching of AuNPs with basic potassium cyanide

Sodium cyanide has played an important role in Au mining and has been the cause of many environmental issues. Both Au and Ag can be dissolved in cyanide solutions. The same methodology can be applied to the etching of NPs [21]. As usual, the large surface area of nanomaterials makes reactions at the surface, in this case, etching kinetically controlled by the surface properties.

For example, treatment of three differently derivatized AuNPs from the same batch behaved quite differently when placed in a solution of 0.1 M of potassium cyanide dissolved in 1.0 M of potassium hydroxide. Table 1 summarizes these results.

Table 1 SPB absorbance remaining after etching of AuNP with basic potassium cyanide.

Surface treated with	Abbreviation	SPB remaining
Untreated	Not applicable	35 %
3-Mercapto-1-propane sulfonic acid, sodium salt	MPSA	85 %
Mercaptohexadecanoic acid	MHDA	69 %

It is clear from Table 1 that unprotected AuNPs are far more reactive toward cyanide than their derivatized counterparts. Among these, that treated with MPSA reacts more slowly than in the case of MHDA, presumably because of the large concentration of negative charges in the former. Similar etching attenuation by thiols [11] have been reported in the literature [21] for particles made by the citrate method and then derivatized; it would appear that the unprotected particles prepared here are even more reactive than citrate unmodified AuNPs.

Acid etching of the shell in Au/Ag core-shell nanoparticles

Core-shell Au/Ag NPs were prepared in CTAC solution following photodecomposition of **I-2959** in the presence of $HAuCl_4$. In these experiments, the mole fraction of Ag(I) was $x_{Ag} = 0.8$. The NPs that form have an absorption spectrum resembling that of AgNP, but significantly broader, largely the result of a weaker and poorly resolved Au SPB in the 500-nm region of the spectrum. Addition of small aliquots of nitric acid (as shown in Fig. 6) leads to the immediate dissolution of the Ag shell, and when 70 μl are added to a 3-mL sample, the Au SPB becomes evident at 520 nm; further addition of nitric acid does not modify the spectrum to any significant extent.

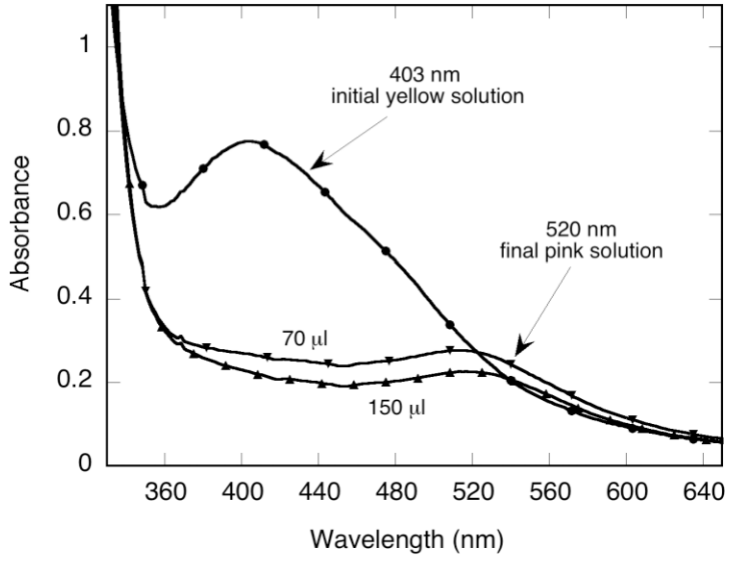

Fig. 6 Spectra for the etching of a self-assembled Au/Ag core-shell NP colloid by concentrated HNO_3. The particles were previously prepared with a total metal ionic concentration of 0.2 mM, molar fraction $x_{Ag} = 0.8$ using stoichiometric amount of **I-2959** and [CTAC] = 0.005 M.

FINAL COMMENTS

The "naked" (or nearly so) NP may be of little interest to a chemist, beyond the challenge to make such materials in a stable form. However, the unprotected surface offers unique opportunities for custom derivatization and for surface reactions. For example, the remarkable seeding growth kinetics of Fig. 5 illustrates the catalytic potential of unprotected nanostructures.

The strategies described here are applicable to other metal ions that are beyond the scope of this article. Such examples include Pt, Co, and Cu. The last two are not noble metals and present additional challenges, since Co and Cu NPs are much more prone to facile oxidation than the bulk materials. Cu, a rather inexpensive material, may find electronic and catalytic applications.

The reduction of Co(II) to form magnetic CoNP can be performed also with α-aminoalkyl radicals, since in this case the radical precursor (**7**) does not reduce Co(II) spontaneously in spite of the presence of the amine functionality [12].

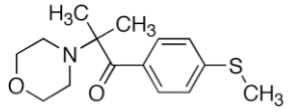

7

The strategies of Scheme 1 and Fig. 3 hold the promise of many new routes for NP synthesis. The spatial and temporal control intrinsic to photoreactions implies that these processes could be performed in situ for imaging, lithographic, or therapeutic applications.

ACKNOWLEDGMENTS

We acknowledge the contribution of many past and present coworkers at the University of Ottawa, whose names appear in the references. Thanks are due to Dr. Yun Liu for her expert help with imaging techniques. This research has been supported by NSERC (Canada), the Canadian Foundation for Innovation, and the Government of Ontario.

REFERENCES

1. L. F. Thompson, C. G. Willson, M. J. Bowden. *Introduction to Microlithography*, American Chemical Society, Washington, DC (1994).
2. M. Brust, M. Walker, D. Bethell, D. J. Schiffrin, R. Whyman. *J. Chem. Soc., Chem. Commun.* 801 (1994).
3. A. Corma, H. Garcia. *Chem. Commun.* 1443 (2004).
4. R. D. Small, J. C. Scaiano. *J. Phys. Chem*. **81**, 828 (1977).
5. J. C. Scaiano. *J. Phys. Chem*. **85**, 2851 (1981).
6. K. L. McGilvray, M. R. Decan, D. Wang, J. C. Scaiano. *J. Am. Chem. Soc.* **128**, 15980 (2006).
7. J. C. Scaiano. *J. Photochem*. **2**, 81 (1973/74).
8. M. V. Encina, E. A. Lissi, E. Lemp, A. Zanocco, J. C. Scaiano. *J. Am. Chem. Soc.* **105**, 1856 (1983).
9. S. Jockusch, M. S. Landis, B. Freiermuth, N. J. Turro. *Macromolecules* **34**, 1619 (2001).
10. N. J. Turro. *Modern Molecular Photochemistry*, p. 628, Benjamin/Cummings, Menlo Park (1978).
11. J. Turkevich, P. C. Stevenson, J. Hiller. *Discuss. Faraday Soc*. **11**, 55 (1951).
12. Unpublished results.
13. E. Gachard, H. Remita, J. Khatouri, B. Keita, L. Nadjo, J. Belloni. *New J. Chem.* **22**, 1257 (1998).
14. J. C. Scaiano, C. Aliaga, S. Maguire, D. Wang. *J. Phys. Chem. B* **110**, 12856 (2006).

15. J. C. Scaiano, E. B. Abuin, L. C. Stewart. *J. Am. Chem. Soc*. **104**, 5673 (1982).
16. H. Paul, R. D. Small Jr., J. C. Scaiano. *J. Am. Chem. Soc*. **100**, 4520 (1978).
17. P. C. Wong, D. Griller, J. C. Scaiano. *J. Am. Chem. Soc.* **104**, 5106 (1982).
18. J. Zheng, P. R. Nicovich, R. M. Dickson. *Annu. Rev. Phys. Chem*. **58**, 409 (2007).
19. T. Vosch, Y. Antoku, J.-C. Hsiang, C. I. Richards, J. I. Gonzalez, R. M. Dickson. *Proc. Natl. Acad. Sci. USA* **104**, 12616 (2007).
20. S. Link, Z. L. Wang, M. A. El-Sayed. *J. Phys. Chem. B* **103**, 3529 (1999).
21. C. S. Weisbecker, M. V. Merritt, G. M. Whitesides. *Langmuir* **12**, 3763 (1996).